Cell

Inactivation of Peroxiredoxin I by Phosphorylation Allows Localized H_2O_2 Accumulation for Cell Signaling

Hyun Ae Woo,[1,*] Sun Hee Yim,[1] Dong Hae Shin,[1] Dongmin Kang,[1] Dae-Yeul Yu,[2] and Sue Goo Rhee[1,*]
[1]Division of Life and Pharmaceutical Sciences, Ewha Womans University, Seoul 120-750, Korea
[2]Aging Research Center, Korea Research Institute of Bioscience and Biotechnology, Daejeon 305-333, Korea
*Correspondence: hawoo@ewha.ac.kr (H.A.W.), rheesg@ewha.ac.kr (S.G.R.)
DOI 10.1016/j.cell.2010.01.009

SUMMARY

Despite its toxicity, H_2O_2 is produced as a signaling molecule that oxidizes critical cysteine residues of effectors such as protein tyrosine phosphatases in response to activation of cell surface receptors. It has remained unclear, however, how H_2O_2 concentrations above the threshold required to modify effectors are achieved in the presence of the abundant detoxification enzymes peroxiredoxin (Prx) I and II. We now show that PrxI associated with membranes is transiently phosphorylated on tyrosine-194 and thereby inactivated both in cells stimulated via growth factor or immune receptors in vitro and in those at the margin of healing cutaneous wounds in mice. The localized inactivation of PrxI allows for the transient accumulation of H_2O_2 around membranes, where signaling components are concentrated, while preventing the toxic accumulation of H_2O_2 elsewhere. In contrast, PrxII was inactivated not by phosphorylation but rather by hyperoxidation of its catalytic cysteine during sustained oxidative stress.

INTRODUCTION

Hydrogen peroxide (H_2O_2) is generated in all aerobic organisms as a byproduct of normal cellular processes. Given that H_2O_2 is toxic to cells, however, such organisms are equipped with detoxifying enzymes such as catalase, glutathione peroxidases (GPxs), and peroxiredoxins (Prxs).

Many mammalian cell types also produce H_2O_2 in response to a variety of extracellular stimuli, with the H_2O_2 so produced serving as a signaling molecule that regulates various biological processes. Stimulation of cells with various agonists thus induces H_2O_2 production, and blockage of H_2O_2 accumulation results in inhibition of signaling by such stimulants (D'Autréaux and Toledano, 2007; Oakley et al., 2009; Rhee, 2006; Xu et al., 2002). For example, in cells stimulated with growth factors such as platelet-derived growth factor (PDGF) or epidermal growth factor (EGF), production of H_2O_2 is required for propagation of growth factor signaling (Bae et al., 1997; Sundaresan et al., 1995). Among the best characterized H_2O_2 effectors are protein tyrosine phosphatases (PTPs): H_2O_2 specifically oxidizes the catalytic cysteine residue of these enzymes and thereby inhibits their activity (Chiarugi and Cirri, 2003; Rhee et al., 2005; Tonks, 2005). Indeed, the activation of protein tyrosine kinases (PTKs) is not sufficient to increase the steady-state level of protein tyrosine phosphorylation in cells; the concurrent inhibition of PTPs by H_2O_2 is also required. Many other H_2O_2 effector molecules also contain an H_2O_2-sensitive cysteine residue.

Evidence indicates that NADPH oxidase (Nox) is largely responsible for receptor-dependent H_2O_2 production (Clempus and Griendling, 2006; Lambeth, 2004; Oakley et al., 2009). Seven distinct catalytic subunits of Nox (Nox1 to Nox5, Duox1, and Duox2) have been identified (Lambeth, 2004). These catalytic subunits are transmembrane proteins and form multisubunit complexes with other membrane as well as cytosolic proteins. Nox generates superoxide by transferring one electron from NADPH to O_2. Superoxide then undergoes dismutation to H_2O_2. Activated Nox complexes appear to assemble within discrete subcellular compartments, including lipid rafts and endosomes, thereby making it possible to produce toxic H_2O_2 molecules within a restricted region of the cell (Li et al., 2006; Oakley et al., 2009; Ushio-Fukai, 2006). For H_2O_2 to serve as a signaling molecule, its concentration must increase rapidly above a certain threshold (10 to 100 μM) and remain elevated long enough for it to oxidize effector molecules (Stone and Yang, 2006). However, in most cells, H_2O_2-eliminating enzymes are present in large concentrations in the cytosol in order to ensure that the toxic molecule remains at low intracellular levels (<0.1 μM) (Stone and Yang, 2006).

PrxI to PrxIV belong to the 2-Cys Prx subfamily of Prx enzymes, which exist as homodimers and reduce H_2O_2 with the use of reducing equivalents provided by thioredoxin (Trx) (Rhee et al., 2005). PrxI and PrxII are localized to the cytosol, whereas PrxIII and PrxIV are restricted to mitochondria and the endoplasmic reticulum, respectively. PrxI and PrxII are also abundant, constituting a total of 0.2% to 1% of soluble protein in cultured mammalian cells (Chae et al., 1999). Catalase is exclusively localized in peroxisomes. GPx1 is present predominantly in the cytosol, but its concentration is smaller than that of PrxI or PrxII in most tissues. Prx enzymes are efficient in eliminating low concentrations of H_2O_2 because of their low K_m

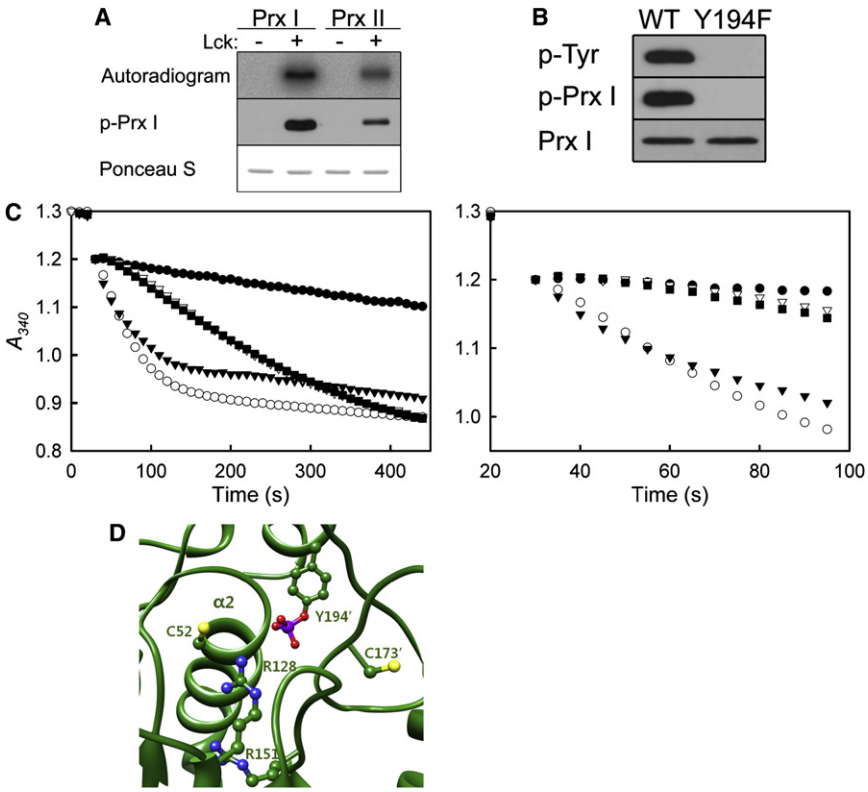

Figure 1. Phosphorylation of PrxI and PrxII In Vitro and Its Effect on the Catalytic Activity of PrxI

(A) Purified recombinant human PrxI or II was subjected to an in vitro kinase assay with Lck in the presence of [γ-^{32}P]ATP. Proteins were separated by SDS-PAGE and visualized by either autoradiography, immunoblot analysis with antibodies to phosphorylated (p-) PrxI, or staining with Ponceau S.

(B) Wild-type (WT) or mutant (Y194F) PrxI expressed in and purified from TKB1 cells was subjected to immunoblot analysis with antibodies to phosphotyrosine (p-Tyr) or to phosphorylated or total PrxI.

(C) Peroxidase activity of nonphosphorylated (open circles) or Tyr^{194}-phosphorylated (closed squares) wild-type PrxI as well as of Y194D (open triangles) or Y194F (closed triangles) mutants of PrxI was monitored in the presence of 50 μM H_2O_2 for 450 s as the decrease in A_{340} by coupling of the reaction to NADPH oxidation (left panel). The initial decrease in A_{340} between 20 and 100 s is expanded in the right panel. NADPH oxidation in the absence of any Prx enzyme (closed circles) was also monitored.

(D) Ribbon diagram of PrxI showing the peroxidatic Cys (Cys^{52}), which is located close to Arg^{128} and Arg^{151} of the same subunit and under the influence of the N-cap effect of helix á2. Phosphorylation of Tyr^{194} in the other subunit of the homodimer introduces a phosphate group (red, oxygen; violet, phosphorus) that is located within a distance of 9 Å from the sulfur atom (yellow) of Cys^{52}. Primed residue numbers correspond to the subunit whose catalytic Cys is not shown.

Additional information is provided in the Extended Experimental Procedures. See also Figure S1.

values for this substrate (Chae et al., 1999). It has therefore remained unclear how, in the presence of PrxI and II, H_2O_2 can accumulate in the cytosol to a concentration sufficient for it to modify target proteins.

The catalytic site of 2-Cys Prxs comprises the NH_2-terminal region of one subunit and the COOH-terminal region of the other subunit in the homodimer (Rhee et al., 2005). The peroxidatic Cys-SH (C_P-SH) is located in the NH_2-terminal region and is selectively oxidized by H_2O_2 to C_P-SOH, which then reacts with the resolving Cys-SH (C_R-SH) in the COOH-terminal region of the other subunit to form an intermolecular disulfide. The disulfide is reduced by Trx. During catalysis, the C_P-SOH intermediate occasionally undergoes further oxidation by H_2O_2 to C_P-SO_2H before the relatively slow formation of a disulfide with C_R-SH can occur. This hyperoxidation, which results in inactivation of peroxidase activity, is reversed by sulfiredoxin (Biteau et al., 2003; Woo et al., 2003a). Given that bacterial Prxs are resistant to hyperoxidation and that prokaryotes do not express sulfiredoxin, reversible inactivation through hyperoxidation has been proposed to be a eukaryotic adaptation that allows H_2O_2 to accumulate to substantial levels under certain circumstances, thereby facilitating H_2O_2-dependent signaling. This concept has been termed the ''floodgate'' hypothesis (Wood et al., 2003). However, no hyperoxidized PrxI or II was observed in cells stimulated with PDGF (Choi et al., 2005).

We have now found that PrxI is phosphorylated on Tyr^{194} and is thereby inactivated in cells stimulated via receptors for growth factors such as PDGF or EGF or via immune receptors such as T cell (TCR) and B cell (BCR) receptors. This phosphorylation is confined to PrxI molecules associated with cell membranes; it was not observed with PrxI present in the cytosol. The spatially confined inactivation of PrxI thus provides a means for generating favorable H_2O_2 gradients around a submembrane compartment, where signaling proteins are concentrated, while minimizing the general accumulation of H_2O_2 to toxic levels and disturbance of global redox potential.

RESULTS

Tyrosine Phosphorylation and Inactivation of PrxI In Vitro

To determine whether Prxs are phosphorylated, we subjected recombinant human PrxI and II to an in vitro kinase assay with two nonreceptor PTKs, Lck and Abl, in the presence of [γ-^{32}P]ATP. Both PTKs phosphorylated PrxI and PrxII, with the extent of phosphorylation for the former being markedly greater than that for the latter (Figure 1A, Figure S1A available online). Tyrosine-194 of PrxI was one of 600 phosphorylation sites revealed by a large-scale proteomic analysis in a cancer cell line treated with pervanadate (Rush et al., 2005). We therefore generated antibodies to Tyr^{194}-phosphorylated PrxI by injection

with a phosphopeptide (KSKEpYFSKQK) corresponding to residues 190 to 199 of PrxI. The sequence SKEYFSK is conserved between PrxI and II. The extents of PrxI and PrxII phosphorylation detected by immunoblot analysis with the phospho-specific antibodies was similar to that revealed by measurement of ^{32}P radioactivity, indicative of similar reactivities of the antibodies for the phosphorylated isozymes. To verify the phosphorylation site of PrxI, we expressed wild-type PrxI or a Tyr^{194} to Phe mutant (Y194F) in the PTK-expressing *Escherichia coli* strain TKB1. Phosphorylation of the wild-type protein was detected, whereas that of the Y194F mutant was not (Figure 1B), indicating that Tyr^{194} is the only site of tyrosine phosphorylation.

We next investigated the effect of phosphorylation of PrxI on its peroxidase activity by subjecting PrxI produced in TKB1 bacteria to affinity chromatography with an immobilized monoclonal antibody to phosphotyrosine (4G10) in order to separate phosphorylated and nonphosphorylated proteins. The peroxidase activity of phosphorylated and nonphosphorylated forms of PrxI was then monitored in the presence of 50 μM H_2O_2 by coupling the peroxidase reaction to NADPH oxidation. After a lag time of ~50 s, the reaction rate for phosphorylated PrxI achieved a steady state that was approximately one-seventh of that for nonphosphorylated PrxI (Figure 1C). No lag time was observed for nonphosphorylated PrxI. The reaction rate for nonphosphorylated PrxI decreased slightly with time because C_P-SH becomes hyperoxidized during catalysis (see below), and the rate became zero when A_{340} reached 0.9 because of exhaustion of H_2O_2 (Figure 1C). A similar lag time (~20 s) and reduced activity (approximately one-fourth of that for nonphosphorylated PrxI) were observed for phosphorylated PrxI when the H_2O_2 concentration was increased to 500 μM (Figure S1B). These results suggest that, at H_2O_2 concentrations in the low micromolar range, the lag time for phosphorylated PrxI would be substantially greater than 50 s and the steady-state reaction rate would be much less than one-seventh of that for the nonphosphorylated enzyme.

The catalytic C_P-SH of PrxI is highly reactive with H_2O_2, because it is surrounded by Arg^{128} and Arg^{151} that stabilize the thiolate anion (C_P-S^-), which is more readily oxidized by H_2O_2 than is its protonated thiol counterpart. Structural modeling predicted that the phosphate moiety of phospho-Tyr^{194} of one subunit of the PrxI homodimer is positioned within 9 Å of the sulfur atom of C_P-SH (Cys^{52}) of the other subunit (Figure 1D). The negatively charged phosphate group might thus be expected to impair the deprotonation of C_p-SH and thereby to decrease its reactivity with H_2O_2. However, after C_P-SH has entered the catalytic cycle, reduction by Trx may return the C_P residue to a state that is not affected to the same extent by the phosphate moiety and that is slightly more reactive with H_2O_2, resulting in a catalytic activity for the phosphorylated enzyme that is reduced but measurable. In support of this notion, a PrxI mutant in which Tyr^{194} is replaced by Asp (Y194D), which therefore contains a negatively charged carboxyl group at position 194, exhibited an activity time course similar to that for phosphorylated PrxI, whereas neutral replacement of the same residue by Phe did not substantially affect enzyme activity (Figure 1C). Comparison of the structures of PrxI and PrxII might also suggest an explanation for the observed slower phosphorylation of PrxII. His^{197} of PrxII appears to form a hydrogen bond with Asp^{181}, with this interaction possibly hindering access of a PTK to Tyr^{193} (the residue corresponding to Tyr^{194} of PrxI) (Figure S1C). No analogous interaction is apparent in PrxI, in which Gln is present at the position corresponding to His^{197} of PrxII.

Tyrosine Phosphorylation of PrxI in Cells Stimulated with Growth Factors

With the antibodies specific for Tyr^{194}-phosphorylated PrxI, we next examined whether PrxI or PrxII is phosphorylated in cells. PrxI and PrxII, which differ by one amino acid residue in size, cannot be separated by SDS-PAGE. Immunoblot analysis revealed that stimulation of rat smooth muscle cells with PDGF resulted in the transient phosphorylation of PrxI or II (Figure 2A). Similar time-dependent phosphorylation of PrxI or II was observed in NIH 3T3 cells stimulated with PDGF (Figure S2A), HER (NIH 3T3 cells that stably express EGF receptor) stimulated with PDGF or EGF (Figure 3, Figure S2B), A431 cells stimulated with EGF (see Figure 4), Ramos B cells stimulated with antibodies to IgM (see Figure 4), and Jurkat T cells stimulated with antibodies to CD3 (see Figure 4). Stimulation of mouse embryonic fibroblasts (MEFs) derived from wild-type or PrxI knockout mice with PDGF yielded a phosphorylated Prx band with the former cells but not with the latter (Figure 2B), suggesting that PrxI is the primary target for growth factor-induced phosphorylation.

Nox1 is the major catalytic subunit of Nox in keratinocytes (Valencia and Kochevar, 2008). We compared PrxI phosphorylation in primary keratinocytes prepared from mice deficient in Nox1 and their wild-type littermates. The extent of PrxI phosphorylation measured 2 min after the onset of stimulation with EGF and PDGF was reduced by ~60% in the Nox1-deficient cells compared with that in the wild-type cells (Figure 2C), suggesting that H_2O_2 generated by Nox1 augments the growth factor-induced inactivation of PrxI, which in turn promotes further accumulation of H_2O_2. This difference was reduced to ~35% and ~25%, respectively, at 5 and 10 min after exposure to PDGF and EGF.

Two-dimensional (2D) PAGE separates not only PrxI and PrxII but also their phosphorylated and nonphosphorylated forms. 2D-PAGE and subsequent immunoblot analysis with antibodies to PrxI or to PrxII revealed that the intensity of spots corresponding to the phosphorylated forms of PrxI or PrxII was too low to be measured in PDGF-stimulated NIH 3T3 cells (data not shown). However, stimulation of the cells with PDGF in the presence of pervanadate resulted in a measurable increase in the amount of phosphorylated PrxI, which accounted for ~5% of total PrxI (Figure S2C); phosphorylated PrxII was still not detected. On the basis of comparison with the one-dimensional immunoblot intensities obtained for cells stimulated with PDGF in the presence of pervanadate, the extent of PrxI phosphorylation in NIH 3T3 cells stimulated with PDGF alone was estimated to be 0.2% to 0.4% of total PrxI (Figure S2D).

Hyperoxidation of C_P-SH to C_P-SO_2H is another mechanism of PrxI inactivation that has been suggested to serve a signaling function (Rhee, 2006; Wood et al., 2003). We therefore next examined the relation between hyperoxidation and phosphorylation of PrxI or II in cells stimulated with growth factors.

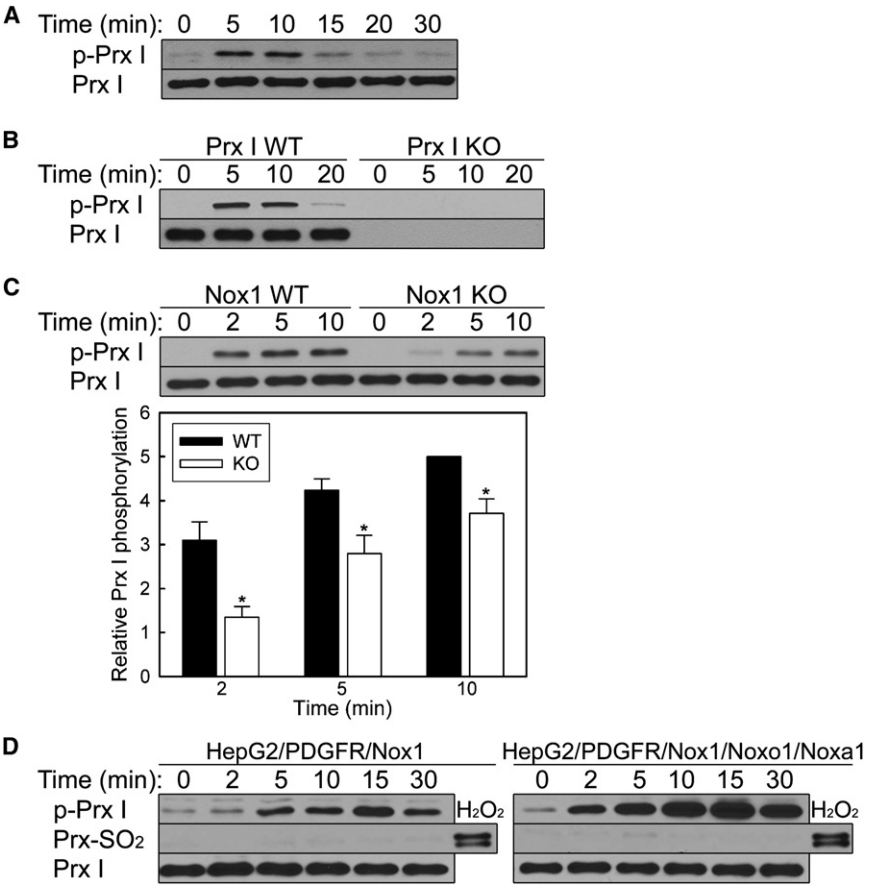

Figure 2. Tyrosine Phosphorylation of PrxI in Growth Factor-Stimulated Cells and the Role of Nox

(A and B) Rat smooth muscle cells (A) or MEFs from wild-type (WT) or PrxI knockout (KO) mice (B) were deprived of serum and then stimulated with PDGF (25 ng/ml) for the indicated times, after which cell lysates (25 μg protein) were subjected to immunoblot analysis with antibodies to phosphorylated or total PrxI.

(C) Keratinocytes isolated from wild-type or Nox1 knockout mice were deprived of serum and then stimulated with EGF (50 ng/ml) and PDGF (25 ng/ml) in the presence of 5 μM sodium pervanadate for the indicated times, after which cell lysates were analyzed as in (A) and (B) (upper panel). The relative extent of PrxI phosphorylation was estimated from the immunoblot band intensities (lower panel); data are presented as mean ± standard error of the mean (SEM) from five independent measurements. *$p < 0.01$ versus corresponding wild-type value.

(D) HepG2 cells stably expressing PDGFR and Nox1 were transfected with expression vectors for Noxo1 and Noxa1 (right) or with the corresponding empty vectors (left), deprived of serum, and then stimulated with PDGF (25 ng/ml) in the presence of 2 μM sodium pervanadate for the indicated times. Cell lysates (20 μg protein) were subjected to immunoblot analysis with antibodies to phosphorylated or total PrxI or to hyperoxidized 2-Cys Prxs (Prx-SO_2). Lysates (5 μg protein) of cells exposed to 1 mM H_2O_2 for 10 min were similarly analyzed as a positive control for Prx hyperoxidation (right-most lanes).

See also Figure S2.

Immunoblot analysis of PDGF-stimulated rat smooth muscle cells or NIH 3T3 cells with antibodies specific for hyperoxidized 2-Cys Prxs did not detect hyperoxidized PrxI or II. We then increased the extent of PDGF-induced H_2O_2 generation in HepG2 cells by overexpressing the PDGF receptor (PDGFR), Nox1, and two additional proteins (Noxo1 and Noxa1) that are necessary for activation of Nox1. The enhanced signaling attributable to the increased H_2O_2 production in the transfected cells was manifest by an increased level of PDGF-induced phosphorylation of PrxI (Figure 2D) as well as of other proteins such as PDGFR and PLC-γ (data not shown). Such enhanced phosphorylation was the result of increased inhibition of PTPs by the increased amounts of H_2O_2. Even under these conditions, hyperoxidation of PrxI or II was not detected (Figure 2D), suggesting that H_2O_2 produced in response to growth factor stimulation does not induce hyperoxidation of PrxI or PrxII.

To examine whether PrxI inactivation by phosphorylation participates in receptor signaling, we assessed the phosphorylation of PDGFR and PLC-γ in PrxI-deficient MEFs reconstituted with either wild-type or Y194F mutant PrxI (Figure S2E). PLC-γ is known to be phosphorylated by PDGFR after binding to autophosphorylated PDGFR via its SH2 domain. The extent of phosphorylation of both proteins measured at 5, 10, and 15 min after PDGF stimulation was reduced by 20% to 30% in the cells expressing the phosphorylation-resistant mutant PrxI compared with that in the wild-type-expressing cells, suggesting that inactivation of PrxI through Tyr^{194} phosphorylation promotes PDGF-dependent tyrosine phosphorylation of cellular proteins.

To identify the PTK responsible for PrxI phosphorylation, we examined the effects of PTK inhibitors. PrxI associates with Abl (Wen and Van Etten, 1997), which is activated in response to PDGF or EGF stimulation (Plattner et al., 1999). STI571 (imatinib mesylate), a highly specific inhibitor of the kinase activities of Abl and PDGFR (Carroll et al., 1997), blocked the induction of PrxI phosphorylation by PDGF, but not that elicited by EGF, in HER cells (Figure 3A), suggesting that Abl is not the kinase responsible for PrxI phosphorylation. EGF-induced phosphorylation of PrxI in A431 cells was blocked by the EGF receptor (EGFR)-specific inhibitor AG1478 (Figure 3B). Both PDGF-induced (data not shown) and EGF-induced (Figure 3C) PrxI phosphorylation were markedly inhibited by PP1, a specific inhibitor of Src family PTKs. Ligation of PDGFR, EGFR, or BCR triggers signaling pathways mediated by the Src family of nonreceptor PTKs, which are expressed in most cell types. The BCR-dependent phosphorylation of PrxI was also inhibited by PP1 in Ramos cells (Figure 3D). To provide further evidence for the role of Src kinases in PrxI phosphorylation, RNA interference was employed to knockdown c-Src in NIH 3T3 cells. c-Src expression in NIH 3T3 cells transfected with Src small interfering RNA (siRNA) was reduced by ~50% compared to expression in cells

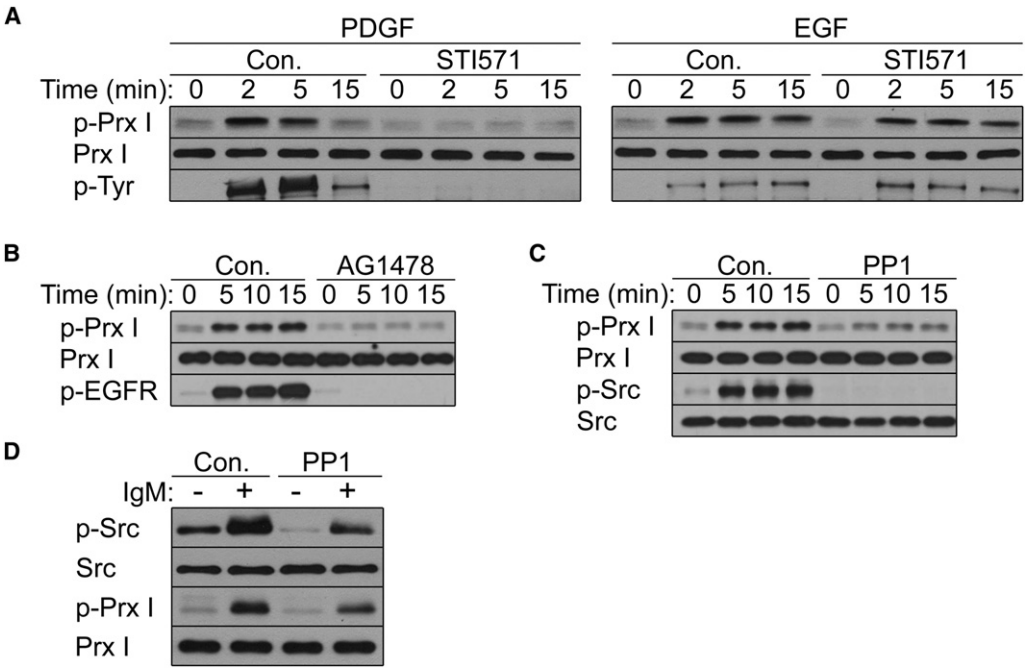

Figure 3. Effects of PTK Inhibitors on PrxI Phosphorylation

(A) Serum-deprived HER cells were incubated for 30 min in the absence (Con.) or presence of 5 μM STI571 and then for the indicated times in the additional presence of PDGF (25 ng/ml) or EGF (50 ng/ml). Cell lysates (25 μg protein) were then subjected to immunoblot analysis with antibodies to phosphorylated or total PrxI or to phosphotyrosine (p-Tyr).

(B and C) Serum-deprived A431 cells were incubated for 30 min in the absence (Con.) or presence of 1 μM AG1478 (B) or 10 μM PP1 (C) and then for the indicated times in the additional presence of EGF (50 ng/ml). Cell lysates (25 μg protein) were then subjected to immunoblot analysis with antibodies to phosphorylated or total forms of PrxI, EGFR, or Src.

(D) Serum-deprived Ramos cells were incubated for 30 min in the absence (Con.) or presence of 10 μM PP1 and then for 5 min in the additional absence or presence of antibodies to IgM (15 μg/ml), after which cell lysates (25 μg protein) were subjected to immunoblot analysis with antibodies to phosphorylated or total forms of Src or PrxI.

See also Figure S3.

transfected with control siRNA (Figure S3). The reduced Src expression was associated with a 25%–50% decrease in PDGF-induced PrxI phosphorylation (Figure S3), supporting the notion that c-Src is at least partly responsible for PrxI phosphorylation in PDGF-stimulated cells.

Phosphorylation of PrxI Associated with Cell Membranes

Nox1 and Nox2 are activated within a submembrane compartment that are characterized by their resistance to nonionic detergents, and both receptor PTKs and Src family kinases are constitutively associated with such domains (Ushio-Fukai, 2006; Oakley et al., 2009). We therefore examined whether the low level of growth factor-induced PrxI phosphorylation (Figure S2D) might reflect restriction of the phosphorylation event to confined area of membranes. Detergent-soluble and -resistant fractions were isolated from A431 cells that had been stimulated with EGF for 5 min and were subjected to immunoblot analysis. The lipid raft-associated protein flotillin 2 (Flot2) (Riento et al., 2009) and phosphorylated PrxI were detected only in the detergent-resistant fraction (Figure 4A). In contrast, PrxI and PrxII were present mostly in the soluble fraction but were also associated with detergent-resistant fraction (Figure 4A), with this association being independent of growth factor stimulation (data not shown). GPx1, another H_2O_2-eliminating enzyme, was detected in the soluble fraction but not in the insoluble fraction (data not shown). Consistent with previous observations (Li et al., 2008), Tyr^{416}-phosphorylated and total forms of Src were detected almost exclusively in the insoluble fraction. Similarly, phosphorylated PrxI was detected only in the insoluble fraction of NIH 3T3 cells stimulated with PDGF (Figure 4B). The compartmentalized phosphorylation of PrxI was also observed in Ramos and Jurkat cells stimulated via BCR and TCR, respectively (Figures 4C and 4D). The TCR is constitutively localized to a submembrane compartment (Miceli et al., 2001), whereas the BCR is translocated to similar compartment in response to its ligation (Cheng et al., 2001). Initial signaling initiated by the two immune receptors is also mediated by members of the Src kinase family.

We monitored the tyrosine phosphorylation of PrxI in A431 cells stimulated with EGF for 0, 1, 3, 5, or 20 min with the use of confocal immunofluorescence microscopy (Figure S4A). The maximal increase was observed at 5 min, after which the extent of phosphorylation decreased. Phosphorylated PrxI in the cells stimulated for 5 min was found to colocalize with Flot2 (Figure 4E).

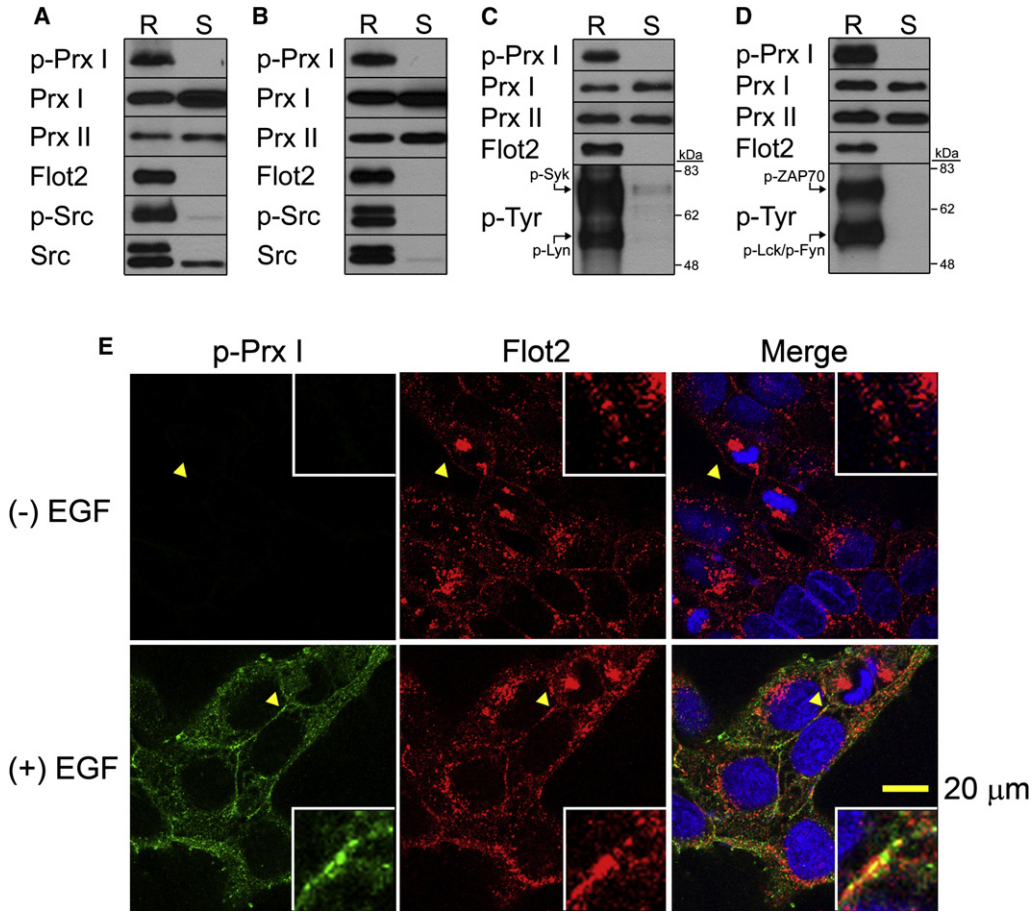

Figure 4. Phosphorylation of PrxI Associated with Confined Membrane Microdomains

(A–D) Serum-deprived A431 cells (A), NIH 3T3 cells (B), Ramos B cells (C), and Jurkat T cells (D) were stimulated for 5 min with EGF (50 ng/ml), PDGF (25 ng/ml), antibodies to IgM (15 μg/ml), or antibodies to CD3 (10 μg /ml), respectively, after which detergent-soluble (S) and -resistant (R) fractions were prepared from cell lysates and subjected to immunoblot analysis with antibodies to the indicated proteins. In (C) and (D), antibodies to phosphotyrosine were used to detect phosphorylated nonreceptor PTKs (p-Syk, p-Lyn, p-ZAP70, p-Lck, and p-Fyn), with the size of molecular markers (in kilodaltons) being indicated on the right.

(E) Serum-deprived A431 cells were incubated for 5 min in the absence or presence of EGF (50 ng/ml), fixed, and subjected to immunofluorescence staining with antibodies to phosphorylated PrxI (green) and to Flot2 (red). Merged images with nuclei stained with 4′,6-diamidino-2-phenylindole (blue) are also shown. The regions indicated by the arrows are shown at higher magnification in the insets. The scale bar represents 20 μm.

See also Figure S4.

To examine whether phosphorylated PrxI colocalizes with activated Nox1, GFP-tagged Noxo1 was transfected into A431 cells. Activation of Nox1 requires translocation of two cytosolic proteins, Noxo1 and Noxa1, to the cell membrane, where Nox1 is embedded. In unstimulated A431 cells expressing GFP-tagged Noxo1, GFP was visualized in the cytosol, and phosphorylated PrxI was not detected. Upon stimulation of the cells with EGF, both GFP and phosphorylated PrxI appeared in the membrane, and the signals for the two proteins colocalized perfectly (Figure S4B).

Phosphorylation of PrxI during Cutaneous Wound Healing

During the process of wound healing, epidermal cells, endothelial cells, and infiltrated immune cells release various growth factors that initiate re-epithelializaton by inducing the migration and proliferation of keratinocytes, fibroblasts, and endothelial cells (Martin, 1997; Singer and Clark, 1999). We therefore investigated whether phosphorylation of PrxI on Tyr^{194} might occur during cutaneous wound repair. The back skin of Balb/c mice was subjected to an incisional injury, and skin tissue was collected at various stages of healing for preparation of protein extracts (Figure S5A). The amount of phosphorylated PrxI increased markedly during the early stage of wound healing, even though the total amount of PrxI decreased in the tissue surrounding the wound area (Figure S5A). We next separated the wound region into the wound edge and the surrounding regenerated area (Figure 5A). Phosphorylation of PrxI was pronounced in the tissue from the wound edge, where growth factors actively promote re-epithelialization, but it was not readily apparent in the tissue from the regenerated area (Figure 5A). The phosphorylation of PrxI at the wound edge was

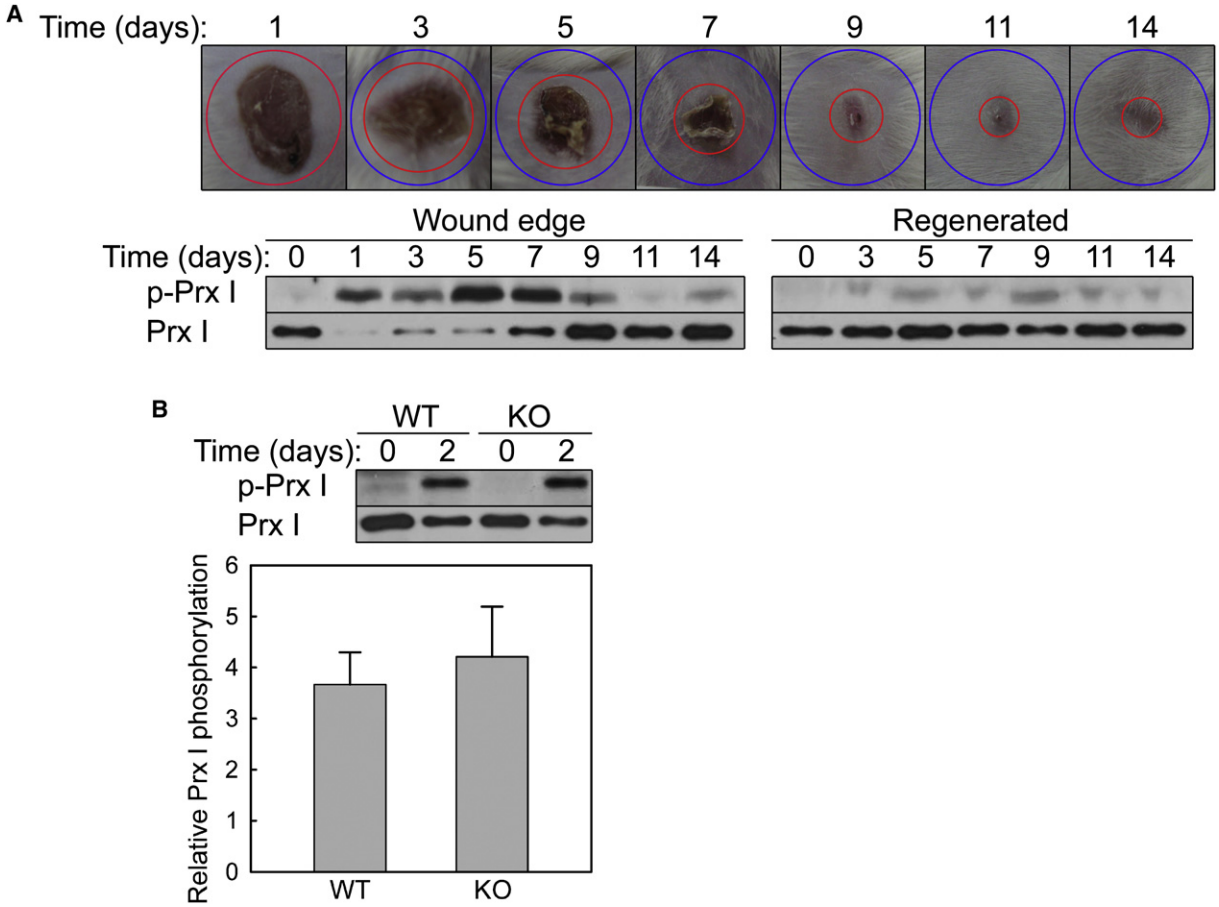

Figure 5. Phosphorylation of PrxI at the Wound Margin during Cutaneous Wound Repair

(A) Balb/c mice were subjected to a full-thickness excisional injury on the back skin, and full-thickness tissue was collected from the areas corresponding to the wound edge (red circle) and the surrounding regenerated region (region between the red and blue circles) at the indicated times thereafter. Protein extracts prepared from the tissue were then subjected to immunoblot analysis with antibodies to phosphorylated or total PrxI.

(B) Protein extracts prepared from the repaired area at 2 days after excisional injury of wild-type or Nox2 knockout mice were subjected to immunoblot analysis as in (A) (upper panel). The relative extent of PrxI phosphorylation was estimated from the band intensities in immunoblots similar to that shown (lower panel); data shown as are mean ± SEM from five independent measurements.

See also Figure S5.

prominent between 1 and 7 days after wounding despite a concomitant marked decrease in the total amount of PrxI. The amount of PrxII in the wound area was also decreased during this same period, whereas that of GPx1 was increased (Figure S5B). The apparent decline in the abundance of both PrxI and PrxII might be due to the introduction of a large amount of proteins such as fibrin from clots at the wound site. The apparent increase in the amount of GPx1 after injury is likely attributable to its high level of expression in infiltrated immune cells compared with that in skin (Figure S5B).

In addition to activating PTKs, growth factors increase H_2O_2 production by various Nox enzymes present in target cells (Lambeth, 2004). Phagocytic cells recruited to the wound site also produce H_2O_2 to kill contaminating bacteria. The increased level of H_2O_2 in the wound fluid, which can achieve micromolar concentrations during the inflammatory phase, facilitates the healing process through redox-sensitive signaling pathways (Sen and Roy, 2008). We therefore examined whether PrxI phosphorylation in the epidermis during wound repair depended on H_2O_2 produced by recruited phagocytic cells. Nox2 is a key source of H_2O_2 in phagocytic cells, and we found that the extent of PrxI phosphorylation in tissue from the wound edge was similar in wild-type and Nox2 knockout mice (Figure 5B), suggesting that H_2O_2 produced by phagocytic cells does not contribute to the observed phosphorylation of PrxI.

Relative Sensitivity of PrxI and PrxII to Hyperoxidation

The peroxidase activity of PrxII in vitro is only 30% of that of PrxI (Chae et al., 1999) (Figure 6A) and is more rapidly extinguished during catalysis as a result of a greater susceptibility of the C_P-SH to hyperoxidation (Figure 6A). We examined the hyperoxidation of PrxI and PrxII in HeLa cells exposed to glucose oxidase in the presence of glucose in order to maintain a steady flux of low levels of H_2O_2. Hyperoxidation, like phosphorylation, results

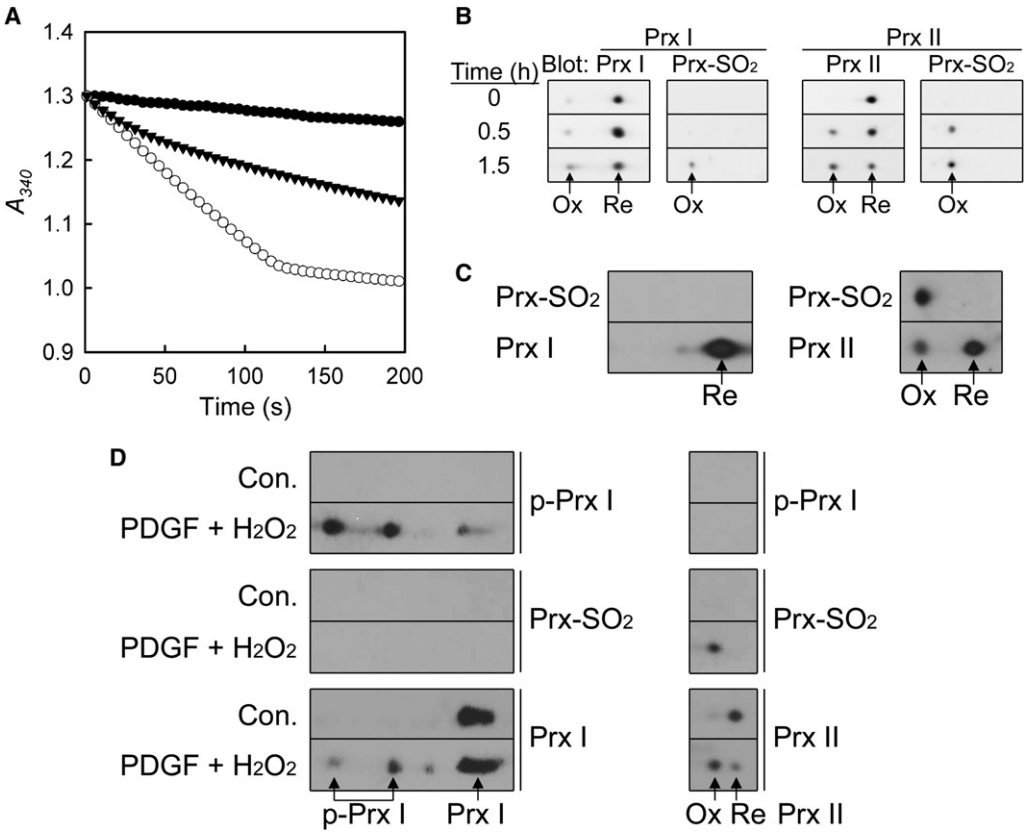

Figure 6. Differential Sensitivity of PrxI and PrxII to Inactivation by Hyperoxidation

(A) The peroxidase activity of 5 μg PrxI (open circles) or 15 μg PrxII (closed triangle) was monitored at 30°C as a decrease in A_{340} by coupling of the reaction to NADPH oxidation in an assay mixture (200 μl) containing 50 mM HEPES-NaOH (pH 7.0), 1 mM EDTA, 300 μM NADPH, 50 nM Trx reductase, 10 μg Trx, and 50 μM H_2O_2. NADPH oxidation in the absence of any Prx enzyme (closed circles) was also monitored.

(B) HeLa cells were incubated for the indicated times with glucose oxidase (30 mU/ml). Cell lysates (250 μg protein) were then analyzed by 2D-PAGE followed by immunoblot analysis with antibodies to PrxI or to PrxII as well as with antibodies specific for hyperoxidized 2-Cys Prxs (Prx–SO_2). Ox and Re indicate oxidized and reduced forms, respectively, of PrxI or II.

(C) Lysates of NIH 3T3 cells that had been exposed to 20 μM paraquat for 8 hr were subjected to 2D-PAGE followed by immunoblot analysis as in (B).

(D) Serum-deprived NIH 3T3 cells were incubated for 15 min in the absence (Con.) or presence of PDGF (25 ng/ml) and 20 μM H_2O_2, after which cell lysates (250 μg protein) were subjected to 2D-PAGE followed by immunoblot analysis as in (B) as well as with antibodies to phosphorylated PrxI. The positions of phosphorylated and nonphosphorylatd PrxI as well as those of oxidized (Ox) and reduced (Re) PrxII are indicated. Tyr^{194}-phosphorylated PrxI is detected at two spots, probably because PrxI undergoes an additional unknown modification when stimulated with PDGF plus H_2O_2.

See also Figure S6.

in an acidic shift of PrxI or II on 2D-PAGE. Exposure of the cells to the generated H_2O_2 for 0.5 or 1.5 hr resulted in the hyperoxidation of ~30% and ~60% of PrxII, respectively, whereas the corresponding values for PrxI were only ~5% and ~10% (Figure 6B). Preferential hyperoxidation of PrxII was also observed in NIH 3T3 cells treated with paraquat (an H_2O_2 generator): whereas ~50% of PrxII was hyperoxidized, PrxI hyperoxidation was not detected (Figure 6C). We then examined the relative sensitivities of PrxI and PrxII to tyrosine phosphorylation and hyperoxidation simultaneously by exposing NIH 3T3 cells to both PDGF and 20 μM H_2O_2 (Figure 6D). PrxI, but not PrxII, was found to undergo phosphorylation, whereas only PrxII underwent hyperoxidation.

This differential susceptibility of PrxI and PrxII to phosphorylation and hyperoxidation suggested that these enzymes might play distinct roles in cell signaling. Hyperoxidation of 2-Cys Prxs results in a structural transition from a dimer to a toroid decamer that can undergo further aggregation, and the decameric and aggregated forms of the enzymes gain protein chaperone function (Jang et al., 2006). Phosphorylation of PrxI on Thr^{90} by a cyclin B-dependent kinase also promotes oligomerization to a decamer (Jang et al., 2006). We therefore determined whether phosphorylation of PrxI on Tyr^{194} might also induce oligomerization. Gel filtration chromatography revealed that phosphorylated PrxI molecules from NIH 3T3 cells stimulated with PDGF existed as dimers, whereas all hyperoxidized PrxI and PrxII in cells exposed to 1 mM H_2O_2 were found in the positions corresponding to decamers (PrxI is also hyperoxidized when cells are exposed to H_2O_2 at 1 mM) (Figure S6). Thus, unlike hyperoxidation and threonine phosphorylation, tyrosine phosphorylation of PrxI does not induce the structural changes that confer chaperone function.

DISCUSSION

Mammalian cells produce H_2O_2 for the purpose of intracellular signaling when stimulated through various cell surface receptors. H_2O_2 is distinct from other messenger molecules in that it acts not by binding to effectors but by oxidizing their critical residues, most notably cysteine, as exemplified by inhibition of PTPs and the tumor suppressor PTEN as a result of oxidation of their catalytic cysteine by H_2O_2 produced in response to stimulation of cells with growth factors (Rhee et al., 2005; Tonks, 2005). It has remained unclear, however, how a toxic molecule like H_2O_2 is able to oxidize effector proteins selectively without inflicting damage on other proteins and lipids. This question has been addressed in part recently by the finding that Nox-dependent production of H_2O_2 molecules for intracellular signaling is localized (Oakley et al., 2009; Ushio-Fukai, 2006).

We have now shown that PrxI becomes phosphorylated on Tyr^{194} in several cell types stimulated via various receptors, including PDGFR, EGFR, BCR, and TCR. Kinetic analysis revealed that phosphorylation of PrxI on Tyr^{194} conferred a long lag time before the onset of peroxidase activity at a reduced level compared with that of the nonphosphorylated enzyme. The lag time was found to be inversely related to the concentration of H_2O_2, suggesting that phosphorylated PrxI would remain inactive as long as H_2O_2 levels around confined membrane microdomains are low. These results indicate that localized production of H_2O_2 might not be sufficient to support the messenger function of this molecule in cells stimulated via growth factor or immune receptors, with inactivation of PrxI by phosphorylation on Tyr^{194} being necessary to protect the pool of H_2O_2 signaling molecules from destruction by this abundant and catalytically efficient enzyme. The absolute amount of Tyr^{194}-phosphorylated PrxI was found to be low because the phosphorylation reaction is confined to PrxI molecules associated with membranes. This selective phosphorylation allows the bulk of PrxI to remain engaged in elimination of H_2O_2 molecules, including those that escape from the site of receptor signaling. Our observation that PrxI phosphorylation was facilitated by Nox1 activation is consistent with the notion that PrxI phosphorylation occurs in the cellular microdomains where H_2O_2 is produced.

The phosphorylation of PrxI on Tyr^{194} was also observed at the wound edge during repair of a cutaneous injury in mice. This finding is likely due to the fact that growth factors such as EGF, PDGF, fibroblast growth factors, transforming growth factor-α, keratinocyte growth factor, and insulin-like growth factor-1 act as key inducers of the proliferation of keratinocytes and fibroblasts at the wound edge (Singer and Clark, 1999). The H_2O_2 produced by infiltrating phagocytic cells is thought to have a beneficial effect on healing by stimulating angiogenesis as well as inducing the tyrosine phosphorylation of focal adhesion kinase (Sen and Roy, 2008). However, the extent of PrxI phosphorylation at the wound edge was not affected by the ablation of Nox2, suggesting that the amount of H_2O_2 released by phagocytic cells at the wound site was not sufficient to increase PrxI phosphorylation. PDGF-induced PrxI phosphorylation was, however, markedly increased by potentiation of H_2O_2 accumulation in HepG2 cells by forced expression of Nox1 and the auxiliary proteins Noxo1 and Noxa1. The role of Nox1-derived H_2O_2 in PrxI phosphorylation was demonstrated again by the observation that the extent of EGF- and PDGF-induced PrxI phosphorylation in primary keratinocytes prepared from mice deficient in Nox1 was reduced by up to ~60% compared with that apparent in wild-type cells. Our results with HepG2 cells and keratinocytes thus suggest that H_2O_2 generated by growth factor-activated Nox1 induces inactivation of PrxI by inactivating PTPs, which in turn promotes the further accumulation of H_2O_2.

A model illustrating the mechanism underlying H_2O_2 accumulation around a submembrane compartment and its role in intracellular signaling is shown in Figure 7. Engagement of a growth factor receptor induces the production of H_2O_2 by activating Nox associated with membranes. At the same time, the activated receptor induces the phosphorylation of cell membrane-associated PrxI on Tyr^{194} by activating a Src family PTK, resulting in inactivation of PrxI, which would otherwise destroy the newly generated H_2O_2. Inactivation of PrxI allows the accumulation of H_2O_2 around a submembrane compartment, which in turn promotes further phosphorylation and inactivation of PrxI both by activating Src kinases and by inactivating PTPs. These two positive feedback loops allow the sustained H_2O_2 signaling necessary for the regulation of biological responses. H_2O_2 is known to activate Src directly by oxidizing its Cys residues or indirectly by inhibiting PTPs (Chiarugi, 2008). The inhibition of PTPs by H_2O_2 is critical for growth factor signaling because activation of receptor PTKs alone is not sufficient to achieve the levels of protein tyrosine phosphorylation necessary for such signaling, with the concurrent inhibition of PTPs by H_2O_2 preventing the futile cycle of phosphorylation and dephosphorylation. Reversible inactivation of PTEN by H_2O_2 is also necessary for signaling mediated by phosphoinositide 3-kinase (Rhee et al., 2005). A similar scenario likely applies to H_2O_2 signaling in cells stimulated via BCR or TCR.

The predisposition of eukaryotic Prxs to hyperoxidation has been proposed to provide a "floodgate" that permits H_2O_2 to accumulate in order to perform its signaling functions (Wood et al., 2003). However, PDGF-induced hyperoxidation of PrxI or II was not observed even when heightened downstream signaling effects of H_2O_2 were apparent, indicating that H_2O_2 produced at cell membranes by Nox does not hyperoxidize PrxI or II and that growth factor signaling does not require inactivation of the two membrane-bound Prxs via hyperoxidation. This finding is consistent with previous observations that normal mitogenic signaling does not require inactivation of 2-Cys Prxs by hyperoxidation (Choi et al., 2005; Phalen et al., 2006). Rather, we found that hyperoxidation of PrxI or II appears to occur as the result of a global increase in the intracellular concentration of H_2O_2, which is consistent with the observation that sulfiredoxin is induced only when cells are exposed to severe oxidative stress (Bae et al., 2009).

Our results show that PrxI and PrxII are regulated differently: PrxI is selectively phosphorylated by PTKs and functions as a modulator of local H_2O_2 levels, whereas PrxII is more susceptible to hyperoxidation in cells subjected to sustained global oxidative stress. Although both PrxI and PrxII are associated with detergent-resistant membranes, inactivation of PrxI, which is more efficient as a peroxidase than PrxII, might be sufficient to allow local accumulation of H_2O_2 for signal propagation. The role

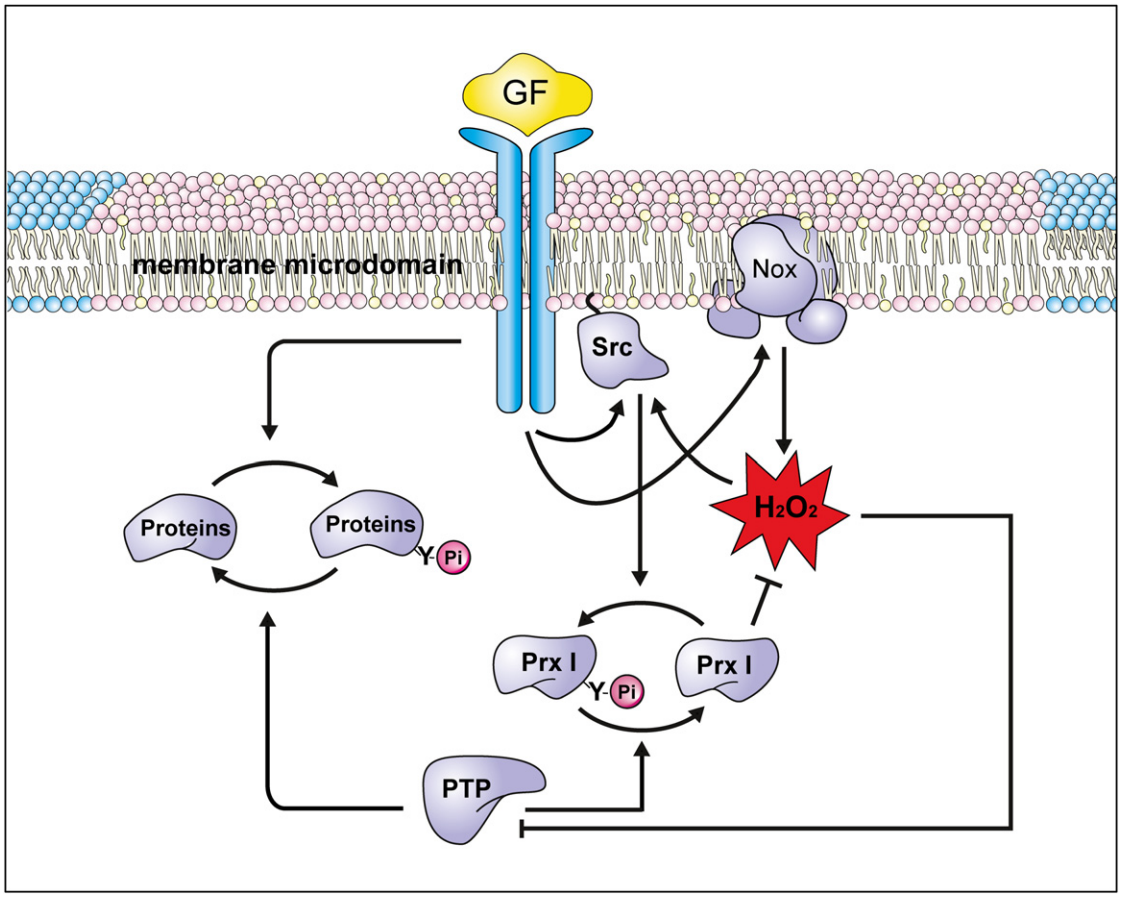

Figure 7. A Model Illustrating the Mechanism Underlying H_2O_2 Accumulation around a Submembrane Compartment and Its Role in Intracellular Signaling

See the Discussion for details. GF, growth factor.

of membrane-associated PrxII remains unclear. Given that the accumulation of a small amount of H_2O_2 at membranes can trigger rapid signal amplification through the action of positive feedback loops (Figure 7), the presence of PrxII in addition to PrxI might function as a safeguard to prevent inappropriate activation of signaling cascades by basal production of H_2O_2 at cell membranes. Consistent with this notion, cells derived from PrxII-deficient mice exhibit enhanced tyrosine phosphorylation of PDGFR when stimulated with PDGF (Choi et al., 2005). Functional differences between PrxI and PrxII are also apparent in the phenotypes of the corresponding knockout mice: mice lacking PrxI thus manifest an increased susceptibility to cancer, whereas those deficient in PrxII do not (Neumann et al., 2003). PrxI has thus been suggested to play a tumor suppressor role, and this suggestion was further supported by the observation that PrxI deficiency in mice increases the susceptibility to Ras- or ErbB-2-induced breast cancer (Cao et al., 2009). Tumor suppression by PrxI was attributed to its ability to bind to PTEN and to protect its lipid phosphatase activity from oxidative inactivation by removing H_2O_2 produced in response to proliferative signals (Cao et al., 2009). PrxII did not bind PTEN (Cao et al., 2009). Given that PrxI activity is critical for maintaining the activation of PTPs and likely PTEN also in the vicinity of the same microdomain, tumor suppression by PrxI is also likely related to its ability to remove H_2O_2 from the region surrounding these microdomains.

EXPERIMENTAL PROCEDURES

Materials

Rabbit antisera specific for PrxI, PrxII, or hyperoxidized 2-Cys Prxs were described previously (Kang et al., 1998; Woo et al., 2003b). Antibodies to EGFR phosphorylated on Tyr^{1068}, to Tyr^{416}-phosphorylated or total forms of Src, or to Flot2 were obtained from Cell Signaling; antibodies to GPx1 were from Young In Frontier; antibodies to human IgM were from Jackson Laboratory; antibodies to phosphotyrosine (4G10), agarose-conjugated 4G10, and recombinant human EGF were from Upstate Biotechnology; antibodies to CD3 was from BD Bioscience; purified recombinant Lck and Abl as well as AG1478 were from Calbiochem; PP1 was from Biomol Research Laboratories; paraquat and glucose oxidase was from Sigma; rat PDGF-BB was from R&D Systems; and STI571 (imatinib mesylate) was from Novartis.

Antibodies to PrxI Phosphorylated on Tyr^{194}

Rabbits were injected with keyhole limpet hemocyanin (Pierce) conjugated to the phosphopeptide KSKEpYFSKQK, which corresponds to residues 190 to 199 of mammalian PrxI. To remove antibodies that recognize the

corresponding nonphosphorylated peptide, we applied serum subsequently obtained from the rabbits to Sepharose 4B resin (GE Healthcare) conjugated with the nonphosphorylated peptide. The unbound fraction was used for immunoblot and immunofluorescence analyses of phosphorylated PrxI or II.

Expression and Purification of PrxI and PrxII

The construction of bacterial expression plasmids for human PrxI and II was described previously (Kang et al., 1998). Mutation of Tyr^{194} of PrxI to aspartate (Y194D) or to phenylalanine (Y194F) was performed with the use of a site-directed mutagenesis kit (Stratagene). Plasmids encoding wild-type PrxI, mutant PrxI, or wild-type PrxII were introduced into *E. coli* BL21(DE3) cells, and the encoded proteins were purified from bacterial extracts as described (Kang et al., 1998).

Cell Culture

A431 cells, HeLa cells, MEFs, as well as HepG2 cells stably expressing PDGFR and Nox1 were maintained under 5% CO_2 at 37°C in Dulbecco's modified Eagle's medium (DMEM) supplemented with 10% fetal bovine serum (FBS), penicillin (100 U/ml), and streptomycin (100 U/ml). NIH 3T3 cells and HER cells (Prywes et al., 1986) were maintained in DMEM supplemented with 10% calf serum, penicillin, and streptomycin. Smooth muscle cells were isolated by enzymatic digestion of the aorta from Sprague-Dawley rats, maintained in DMEM supplemented with 10% FBS, penicillin, and streptomycin, and used for experiments in passages three to five. Keratinocytes were isolated from newborn homozygous Nox1 knockout mice (Matsuno et al., 2005) and genetically matched wild-type controls as described (Lichti et al., 2008); they were cultured in minimal essential medium supplemented with 10% FBS. PrxI knockout mice will be described elsewhere. Ramos cells and Jurkat cells were maintained in RPMI supplemented with 10% FBS, penicillin, and streptomycin.

Isolation of Detergent-Soluble and -Resistant Fractions

A431, NIH 3T3, Ramos, or Jurkat cells were subjected to the procedure of Radeva and Sharom (Radeva and Sharom, 2004) with a slight modification. In brief, stimulated cells (2×10^8 cells) were suspended in 1 ml lysis buffer containing of 0.5% Brij-96 in 25 mM Tris-HCl, 140 mM NaCl, 1 mM EDTA, 1 mM AEBSF, and 1 mM Na_3VO_4. Cells were left on ice for 30 min to lyse and were then centrifuged at 10,000 × g for 5 min to obtain the postnuclear fraction. The postnuclear lysate was adjusted to 40% (w/v) sucrose in the same buffer, and then a 5%–30% discontinuous sucrose gradient was layered on the top. Samples were centrifuged at 36,000 rpm for 20 hr at 4°C with a SW41 rotor (Beckman Coulter). Fractions of 0.8 ml were collected from the top of the gradient tube.

Mouse Model of Cutaneous Wound Repair

Balb/c mice or homozygous Nox2 knockout mice (Jackson Laboratory) and their corresponding wild-type controls (all at 10 to 12 weeks of age) were used for the wounding experiments. All animal experiments were performed according to a protocol approved by the Institutional Animal Care and Use Committee of Ewha Womans University. Mice were anesthetized by intraperitoneal injection of a mixture of tiletamine, zolazepam, and xylazine, and two full-thickness excisional wounds were made on the back skin of the animals with the use of a 6 mm biopsy punch. Wound tissue was collected at various times after wounding, frozen in liquid nitrogen, and subsequently used to prepare protein extracts.

SUPPLEMENTAL INFORMATION

Supplemental Information includes Extended Experimental Procedures and six figures and can be found with this article online at doi:10.1016/j.cell.2010.01.009.

ACKNOWLEDGMENTS

This study was supported by grants from the National Research Foundation of Korea (National Honor Scientist program grant 2009-0052293 and Bio R&D program grant M10642040001-07N4204-00110 to S.G.R.). We thank K. Matsuno and C. Yabe-Nishimura for providing Nox1-deficent mice.

Received: July 24, 2009
Revised: November 6, 2009
Accepted: January 4, 2010
Published: February 18, 2010

REFERENCES

Bae, Y.S., Kang, S.W., Seo, M.S., Baines, I.C., Tekle, E., Chock, P.B., and Rhee, S.G. (1997). Epidermal growth factor (EGF)-induced generation of hydrogen peroxide. Role in EGF receptor-mediated tyrosine phosphorylation. J. Biol. Chem. *272*, 217–221.

Bae, S.H., Woo, H.A., Sung, S.H., Lee, H.E., Lee, S.K., Kil, I.S., and Rhee, S.G. (2009). Induction of sulfiredoxin via an Nrf2-dependent pathway and hyperoxidation of peroxiredoxin III in the lungs of mice exposed to hyperoxia. Antioxid. Redox Signal *11*, 937–948.

Biteau, B., Labarre, J., and Toledano, M.B. (2003). ATP-dependent reduction of cysteine-sulphinic acid by S. cerevisiae sulphiredoxin. Nature *425*, 980–984.

Cao, J., Schulte, J., Knight, A., Leslie, N.R., Zagozdzon, A., Bronson, R., Manevich, Y., Beeson, C., and Neumann, C.A. (2009). Prdx1 inhibits tumorigenesis via regulating PTEN/AKT activity. EMBO J. *28*, 1505–1517.

Carroll, M., Ohno-Jones, S., Tamura, S., Buchdunger, E., Zimmermann, J., Lydon, N.B., Gilliland, D.G., and Druker, B.J. (1997). CGP 57148, a tyrosine kinase inhibitor, inhibits the growth of cells expressing BCR-ABL, TEL-ABL, and TEL-PDGFR fusion proteins. Blood *90*, 4947–4952.

Chae, H.Z., Kim, H.J., Kang, S.W., and Rhee, S.G. (1999). Characterization of three isoforms of mammalian peroxiredoxin that reduce peroxides in the presence of thioredoxin. Diabetes Res. Clin. Pract. *45*, 101–112.

Cheng, P.C., Brown, B.K., Song, W., and Pierce, S.K. (2001). Translocation of the B cell antigen receptor into lipid rafts reveals a novel step in signaling. J. Immunol. *166*, 3693–3701.

Chiarugi, P. (2008). Src redox regulation: there is more than meets the eye. Mol. Cells *26*, 329–337.

Chiarugi, P., and Cirri, P. (2003). Redox regulation of protein tyrosine phosphatases during receptor tyrosine kinase signal transduction. Trends Biochem. Sci. *28*, 509–514.

Choi, M.H., Lee, I.K., Kim, G.W., Kim, B.U., Han, Y.H., Yu, D.Y., Park, H.S., Kim, K.Y., Lee, J.S., Choi, C., et al. (2005). Regulation of PDGF signalling and vascular remodelling by peroxiredoxin II. Nature *435*, 347–353.

Clempus, R.E., and Griendling, K.K. (2006). Reactive oxygen species signaling in vascular smooth muscle cells. Cardiovasc. Res. *71*, 216–225.

D'Autréaux, B., and Toledano, M.B. (2007). ROS as signalling molecules: mechanisms that generate specificity in ROS homeostasis. Nat. Rev. Mol. Cell Biol. *8*, 813–824.

Jang, H.H., Kim, S.Y., Park, S.K., Jeon, H.S., Lee, Y.M., Jung, J.H., Lee, S.Y., Chae, H.B., Jung, Y.J., Lee, K.O., et al. (2006). Phosphorylation and concomitant structural changes in human 2-Cys peroxiredoxin isotype I differentially regulate its peroxidase and molecular chaperone functions. FEBS Lett. *580*, 351–355.

Kang, S.W., Chae, H.Z., Seo, M.S., Kim, K., Baines, I.C., and Rhee, S.G. (1998). Mammalian peroxiredoxin isoforms can reduce hydrogen peroxide generated in response to growth factors and tumor necrosis factor-alpha. J. Biol. Chem. *273*, 6297–6302.

Lambeth, J.D. (2004). NOX enzymes and the biology of reactive oxygen. Nat. Rev. Immunol. *4*, 181–189.

Li, Q., Harraz, M.M., Zhou, W., Zhang, L.N., Ding, W., Zhang, Y., Eggleston, T., Yeaman, C., Banfi, B., and Engelhardt, J.F. (2006). Nox2 and Rac1 regulate H2O2-dependent recruitment of TRAF6 to endosomal interleukin-1 receptor complexes. Mol. Cell. Biol. *26*, 140–154.

Li, Q., Zhang, Y., Marden, J.J., Banfi, B., and Engelhardt, J.F. (2008). Endosomal NADPH oxidase regulates c-Src activation following hypoxia/reoxygenation injury. Biochem. J. *411*, 531–541.

Lichti, U., Anders, J., and Yuspa, S.H. (2008). Isolation and short-term culture of primary keratinocytes, hair follicle populations and dermal cells from newborn mice and keratinocytes from adult mice for in vitro analysis and for grafting to immunodeficient mice. Nat. Protoc. *3*, 799–810.

Martin, P. (1997). Wound healing—aiming for perfect skin regeneration. Science *276*, 75–81.

Matsuno, K., Yamada, H., Iwata, K., Jin, D., Katsuyama, M., Matsuki, M., Takai, S., Yamanishi, K., Miyazaki, M., Matsubara, H., and Yabe-Nishimura, C. (2005). Nox1 is involved in angiotensin II-mediated hypertension: a study in Nox1-deficient mice. Circulation *112*, 2677–2685.

Miceli, M.C., Moran, M., Chung, C.D., Patel, V.P., Low, T., and Zinnanti, W. (2001). Co-stimulation and counter-stimulation: lipid raft clustering controls TCR signaling and functional outcomes. Semin. Immunol. *13*, 115–128.

Neumann, C.A., Krause, D.S., Carman, C.V., Das, S., Dubey, D.P., Abraham, J.L., Bronson, R.T., Fujiwara, Y., Orkin, S.H., and Van Etten, R.A. (2003). Essential role for the peroxiredoxin Prdx1 in erythrocyte antioxidant defence and tumour suppression. Nature *424*, 561–565.

Oakley, F.D., Abbott, D., Li, Q., and Engelhardt, J.F. (2009). Signaling components of redox active endosomes: the redoxosomes. Antioxid. Redox Signal *11*, 1313–1333.

Phalen, T.J., Weirather, K., Deming, P.B., Anathy, V., Howe, A.K., van der Vliet, A., Jönsson, T.J., Poole, L.B., and Heintz, N.H. (2006). Oxidation state governs structural transitions in peroxiredoxin II that correlate with cell cycle arrest and recovery. J. Cell Biol. *175*, 779–789.

Plattner, R., Kadlec, L., DeMali, K.A., Kazlauskas, A., and Pendergast, A.M. (1999). c-Abl is activated by growth factors and Src family kinases and has a role in the cellular response to PDGF. Genes Dev. *13*, 2400–2411.

Prywes, R., Livneh, E., Ullrich, A., and Schlessinger, J. (1986). Mutations in the cytoplasmic domain of EGF receptor affect EGF binding and receptor internalization. EMBO J. *5*, 2179–2190.

Radeva, G., and Sharom, F.J. (2004). Isolation and characterization of lipid rafts with different properties from RBL-2H3 (rat basophilic leukaemia) cells. Biochem. J. *380*, 219–230.

Rhee, S.G. (2006). Cell signaling. H2O2, a necessary evil for cell signaling. Science *312*, 1882–1883.

Rhee, S.G., Kang, S.W., Jeong, W., Chang, T.S., Yang, K.S., and Woo, H.A. (2005). Intracellular messenger function of hydrogen peroxide and its regulation by peroxiredoxins. Curr. Opin. Cell Biol. *17*, 183–189.

Riento, K., Frick, M., Schafer, I., and Nichols, B.J. (2009). Endocytosis of flotillin-1 and flotillin-2 is regulated by Fyn kinase. J. Cell Sci. *122*, 912–918.

Rush, J., Moritz, A., Lee, K.A., Guo, A., Goss, V.L., Spek, E.J., Zhang, H., Zha, X.M., Polakiewicz, R.D., and Comb, M.J. (2005). Immunoaffinity profiling of tyrosine phosphorylation in cancer cells. Nat. Biotechnol. *23*, 94–101.

Sen, C.K., and Roy, S. (2008). Redox signals in wound healing. Biochim. Biophys. Acta *1780*, 1348–1361.

Singer, A.J., and Clark, R.A. (1999). Cutaneous wound healing. N. Engl. J. Med. *341*, 738–746.

Stone, J.R., and Yang, S. (2006). Hydrogen peroxide: a signaling messenger. Antioxid. Redox Signal. *8*, 243–270.

Sundaresan, M., Yu, Z.X., Ferrans, V.J., Irani, K., and Finkel, T. (1995). Requirement for generation of H2O2 for platelet-derived growth factor signal transduction. Science *270*, 296–299.

Tonks, N.K. (2005). Redox redux: revisiting PTPs and the control of cell signaling. Cell *121*, 667–670.

Ushio-Fukai, M. (2006). Localizing NADPH Oxidase-derived ROS. Science's Stke, http://www.stke.org/cgi/content/full/2006/349/re8.

Valencia, A., and Kochevar, I.E. (2008). Nox1-based NADPH oxidase is the major source of UVA-induced reactive oxygen species in human keratinocytes. J. Invest. Dermatol. *128*, 214–222.

Wen, S.T., and Van Etten, R.A. (1997). The PAG gene product, a stress-induced protein with antioxidant properties, is an Abl SH3-binding protein and a physiological inhibitor of c-Abl tyrosine kinase activity. Genes Dev. *11*, 2456–2467.

Woo, H.A., Chae, H.Z., Hwang, S.C., Yang, K.S., Kang, S.W., Kim, K., and Rhee, S.G. (2003a). Reversing the inactivation of peroxiredoxins caused by cysteine sulfinic acid formation. Science *300*, 653–656.

Woo, H.A., Kang, S.W., Kim, H.K., Yang, K.S., Chae, H.Z., and Rhee, S.G. (2003b). Reversible oxidation of the active site cysteine of peroxiredoxins to cysteine sulfinic acid. Immunoblot detection with antibodies specific for the hyperoxidized cysteine-containing sequence. J. Biol. Chem. *278*, 47361–47364.

Wood, Z.A., Poole, L.B., and Karplus, P.A. (2003). Peroxiredoxin evolution and the regulation of hydrogen peroxide signaling. Science *300*, 650–653.

Xu, D., Rovira, I.I., and Finkel, T. (2002). Oxidants painting the cysteine chapel: redox regulation of PTPs. Dev. Cell *2*, 251–252.